

# Transmission Characteristics on Composite Right/Left-Handed Cylindrical Waveguides Constructed by the Cutoff TE and TM Modes

Shigeyuki Nishimura, Hiroyuki Deguchi, and Mikio Tsuji\*

**Abstract**—This paper proposes a composite right/left-handed cylindrical waveguide. Negative permeability is realized by the cutoff  $TM_{01}$ -mode in a hollow waveguide, and negative permittivity is realized by the cutoff dominant TE-mode in a sector waveguide with a ridge. Usefulness of the proposed cylindrical waveguide is verified from the numerical computations of both the dispersion diagrams and the transmission characteristics of the structure with finite-number unit cells. Finally, measurement of the fabricated waveguides is performed for the experimental verification.

## 1. INTRODUCTION

Metamaterial which is an artificial medium having simultaneously equivalent negative permittivity and negative permeability has recently received a lot of attention. In 1968, Veselago inspected metamaterials theoretically in which a backward wave transmits [1], and then in 2000, Smith et al. experimentally realized a metamaterial by using a split-ring resonator [2]. To date, graphene is investigated as one of the promising metamaterials for application [3, 4]. On the other hand, to realize left-handed nature on a transmission line, a composite right/left-handed transmission line (CRLH-TL) which adds both a series capacitor and a shunt inductor to the original line was first proposed [5]. Then CRLH-TLs consisting of various shapes have been reported [6–19]. Left-handed waveguides are constructed by loading capacitive shorted stubs and inductive windows in [6, 7], and also by inserting corrugations [8–11]. Furthermore, these waveguides are realized by combining TE evanescent mode with the negative-permeability component [12, 13] and by combining TM evanescent mode with the negative-permittivity component [14]. The left-handed waveguide constructed by only metal waveguides has been proposed by using the cutoff TE-mode and cutoff TM-mode indicating negative permittivity and negative permeability, respectively [20–24].

In this paper, the transmission characteristics of the partially ridge-loaded composite right/left-handed cylindrical waveguide proposed by us [21–23] are investigated on a ridge shape in detail, and the composite nature is confirmed experimentally. The proposed waveguide is easily constructed by connecting two circular waveguides having different cross sections. This corresponds to combining the section with negative permeability based on the cutoff  $TM_{01}$  mode and the section with negative permittivity based on the cutoff dominant TE mode in a sector waveguide. The field distributions of these modes are almost similar, so that matching between these sections is very good. Furthermore, to achieve a balanced condition without band gap between the left-handed and right-handed pass bands, a square conductor ridge is introduced in the center of the sector waveguide, thereby adjusting the cutoff frequency of the dominant TE mode. In the numerical calculation by HFSS, dispersion diagrams of the CRLH-TL and transmission characteristics of the structure with the finite-number unit cells are

---

*Received 30 May 2018, Accepted 12 July 2018, Scheduled 21 August 2018*

\* Corresponding author: Mikio Tsuji (mtsuji@mail.doshisha.ac.jp).

The authors are with the Department of Electronics, Doshisha University, Kyotanabe, Kyoto 610-0321, Japan.

investigated by varying the structural parameters. Finally, we fabricate the proposed CRLH-TL and compare its transmission characteristics between the measured and numerical results.

## 2. CONSTRUCTION OF LEFT-HANDED WAVEGUIDE

Figures 1(a), (b) and (c) show field distributions of the dominant  $TE_{11}$  and higher-order  $TM_{01}$  modes, and their dispersion characteristics in a hollow cylindrical waveguide with the radius  $r = 10.12$  [mm], respectively. When a coaxial line is used as input/output waveguides, the field distribution of its dominant TEM mode is very similar to that of  $TM_{01}$  mode as shown in Fig. 1(b). As a result,  $TM_{01}$  mode can be mainly excited by the coaxial line. If  $TM_{01}$  mode is below cutoff, the waveguide has equivalent negative-permeability medium which can be expressed as a series capacitor. On the other hand, the field distribution of the dominant  $TE_{11}$  mode is greatly different from that of  $TM_{01}$  mode, and yet, the former cutoff frequency is lower than the latter one as shown in Fig. 1. Therefore, to realize negative permittivity medium based on the cutoff dominant TE mode, the cylindrical waveguide has to be modified. We propose here to introduce the dominant TE mode in a sector cylindrical waveguide which is divided into  $N$  sections by thin conductor walls. Fig. 2(a) shows their dispersion characteristics for various  $N$  for the conductor-wall thickness  $d = 2$  [mm]. We can see that increase of the dividing number  $N$  makes the cutoff frequency of the dominant TE mode higher. When we take  $N = 4$ , its cutoff frequency is higher than that of the  $TM_{01}$  mode, and its field distribution is almost similar to that of  $TM_{01}$  mode as shown in Fig. 2(b).

This fact brings that both modes may be transformed to each other with less mismatching on the connection plane between the TM and TE waveguides. However, the cutoff frequencies between  $TM_{01}$

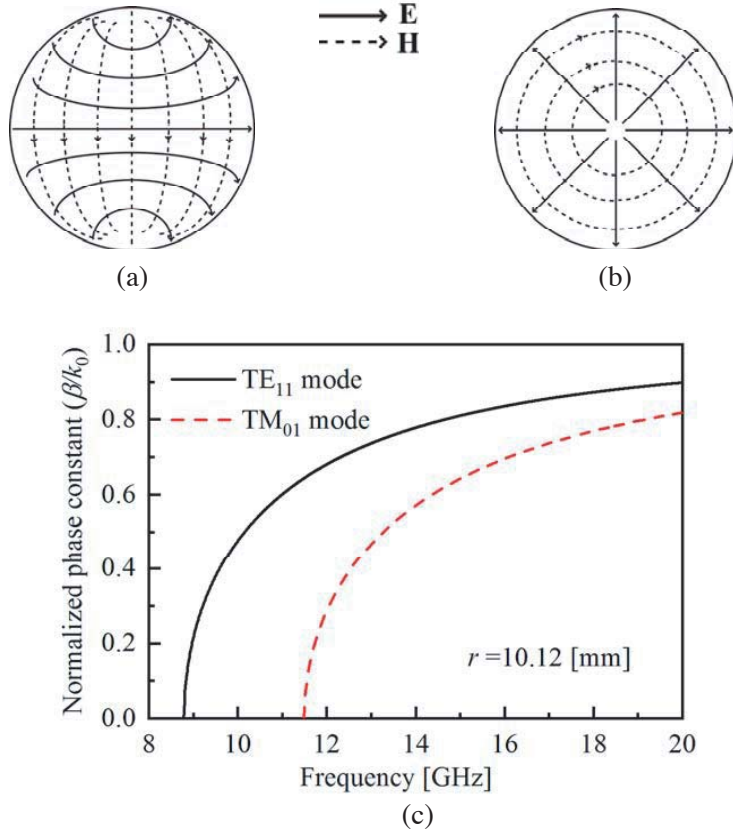


**Figure 1.** Field distributions of (a) the dominant  $TE_{11}$  mode and (b) the next higher-order  $TM_{01}$  mode on the cylindrical waveguide with the radius  $r = 10.12$  [mm], and their dispersion characteristics  $\beta/k_0$ . ( $\beta$  is the phase constant and  $k_0$  is the wavenumber in the free space.)

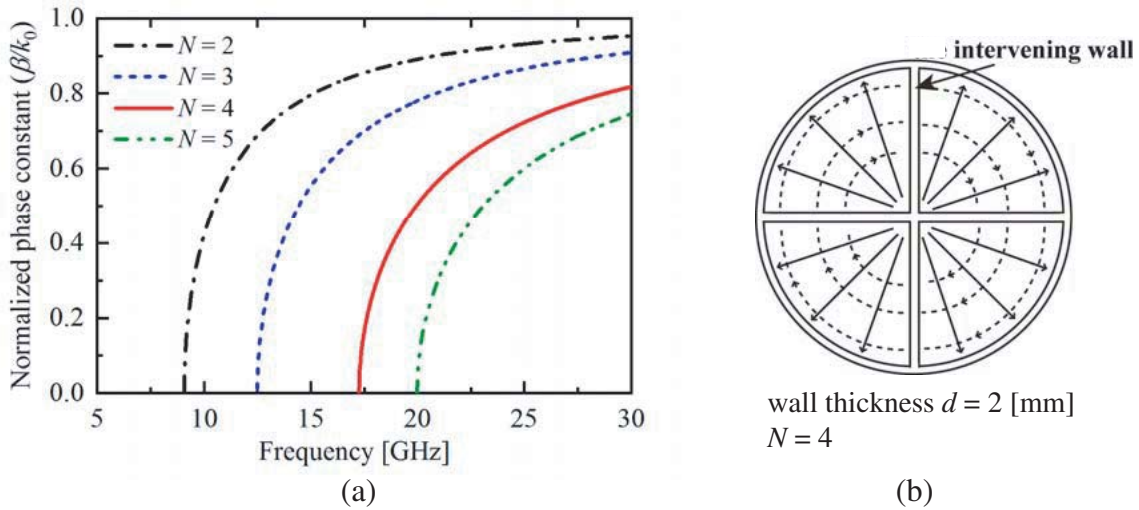


**Figure 2.** (a) Dispersion characteristics  $\beta/k_0$  of the dominant TE modes on the  $N$ -divided sector waveguide with the radius  $r = 10.12$  [mm], and (b) filed distributions of the dominant TE mode for  $N = 4$ .

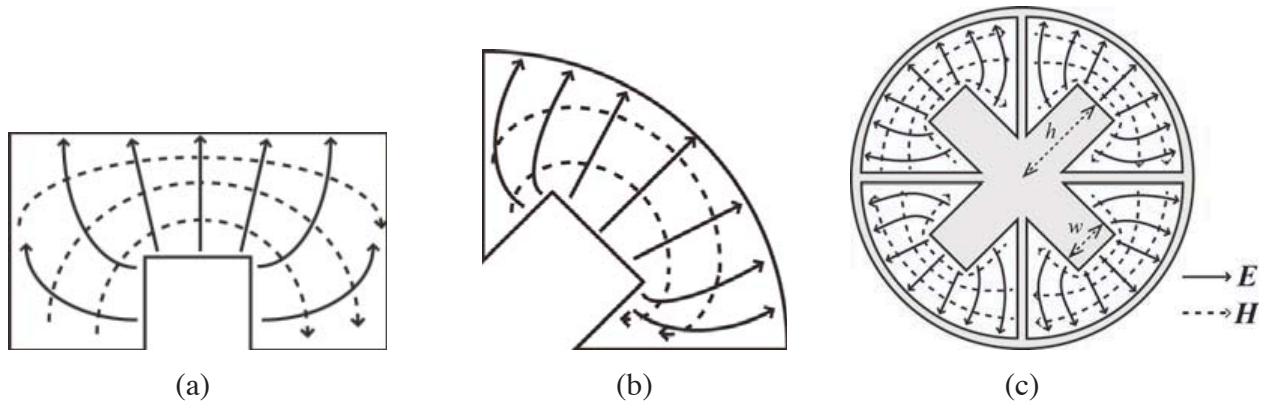


**Figure 3.** Distributions of the electromagnetic field on the waveguide loading a ridge. (a)  $TE_{10}$  mode (rectangular waveguide), (b) the dominant TE mode (sector waveguide), and (c) the dominant TE mode (4-divided cylindrical waveguide).

mode and the dominant TE mode cannot be equal to each other only by the division. So we introduce a ridge in the center of the sector guide. The effect is the same with the ridge installed in the rectangular waveguide as shown in Fig. 3. That is, the cutoff frequency of the dominant TE mode can be lowered by the ridge effect. Figs. 4(a), (b), and (c) show the dispersion characteristics of the dominant TE mode in the 4-divided sector waveguide for dependence of the ridge height  $h$ , ridge width  $w$ , and wall thickness  $d$ , respectively. We can see from this figure that the dispersion characteristic of the dominant TE mode strongly depends on the ridge height  $h$  and wall thickness  $d$ , whereas it does not depend on the ridge width  $w$  so much. The trend of the dispersion characteristics for parameters  $h$  and  $d$  can be explained by the additional shunt capacitance due to the ridge and variation of the waveguide space due to the wall thickness, respectively. So we select ridge height  $h$  as a parameter controlling the cutoff frequency of the dominant TE mode. As a result, it is possible to construct the waveguide section with negative permittivity which expresses a shunt inductor in the same frequency range with the cutoff  $TM_{01}$ -mode waveguide section with negative permeability. Therefore, the composite right/left-handed waveguide is constructed by combining these sections alternatively.

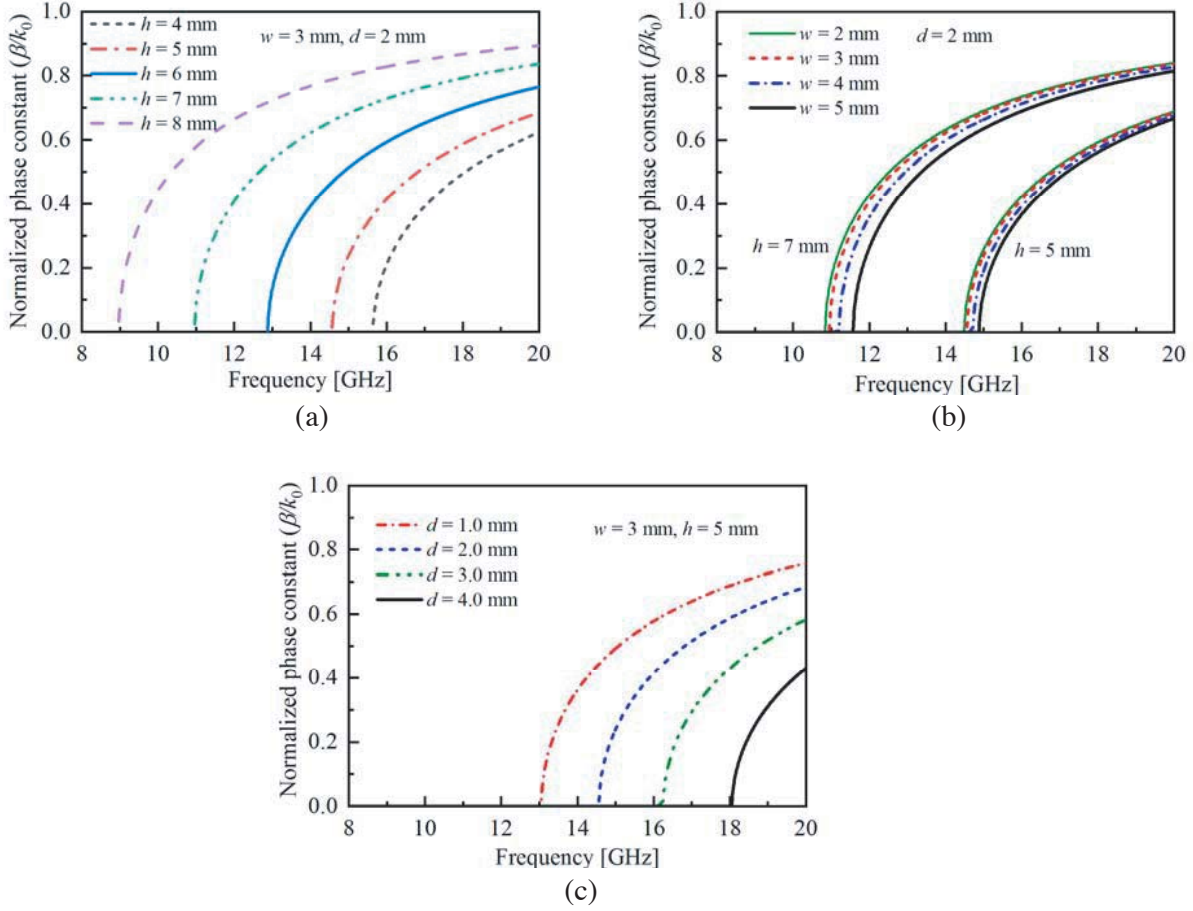


**Figure 4.** Dispersion characteristics of the dominant TE mode for various (a) ridge height  $h$ , (b) ridge width  $w$  and (c) wall thickness  $d$ .

### 3. ANALYTICAL RESULTS

#### 3.1. Structure of the CRLH-TL

The unit cell of the proposed CRLH-TL is shown in Fig. 5. The ridge width  $w$  and wall thickness  $d$  are fixed at 3 mm and 2 mm, respectively. The lengths of TE-mode and TM-mode sections are  $l_1$  and  $l_2$ . The radii of the cylindrical waveguide in the two sections are equal to each other. A hollow coaxial line which has the same outer radius and characteristic impedance  $50 \Omega$  (the inner radius 4.1 mm) is used as input and output waveguides. In the following section, dispersion diagram is derived from the Bloch-Floquet theorem under consideration of the higher-order modal coupling between adjacent unit cells [25], and transmission characteristic is calculated for the guide with the finite 12 unit cells.

#### 3.2. Effects of the Structural Parameters

Figure 6 shows the dispersion diagram  $\beta l$  ( $l = l_1 + l_2$ : the unit-cell length) for various heights of ridge  $h$ , when  $l_1 = 1.0$  [mm] and  $l_2 = 10.0$  [mm]. It is found from this figure that the left-handed passband region is formed in the lower-frequency side, while the right-handed passband region is formed in the higher-frequency side. The band gap exists between both the passbands. In the case of  $h = 4.7$  [mm], the balanced condition in which the band gap disappears is realized. For ridge height  $h$  more than 4.7 mm, the band gap extends from the frequency at the balanced point to the lower frequency side, whereas for  $h$  less than 4.7 mm, it extends from the frequency at the balanced point to the higher frequency side. This is caused by the fact that the cutoff frequency of the TE dominant mode moves

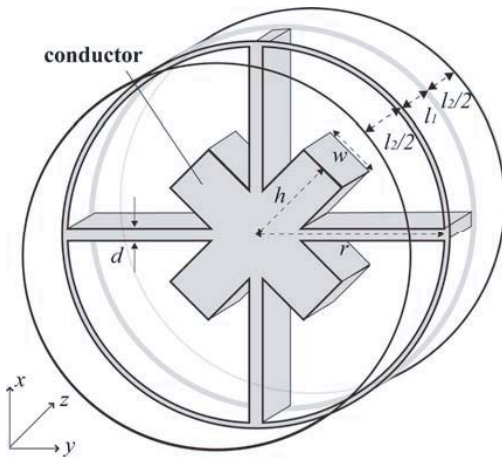


**Figure 5.** Unit-cell structure of the proposed CRLH cylindrical waveguide.

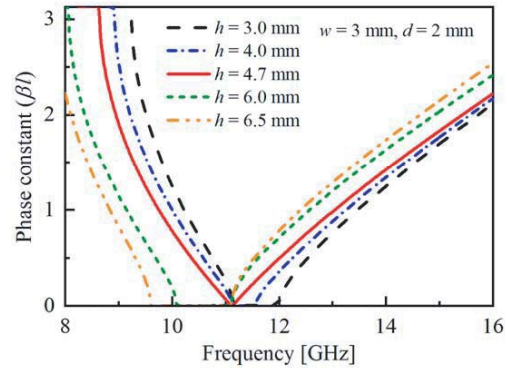


**Figure 6.** Dispersion diagrams of the CRLH cylindrical waveguide for various ridge height  $h$  in the case of  $l_1 = 1.0$  [mm] and  $l_2 = 10.0$  [mm].

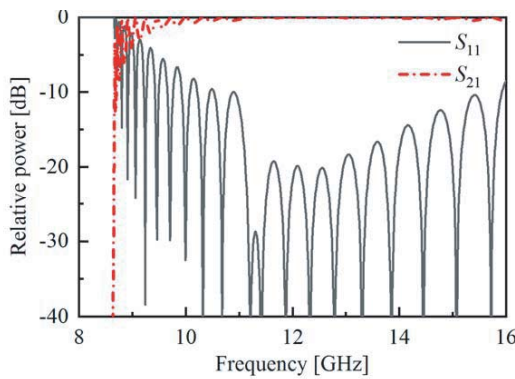


**Figure 7.** Transmission characteristics for 12 unit cells in the case of  $h = 4.7$  [mm].

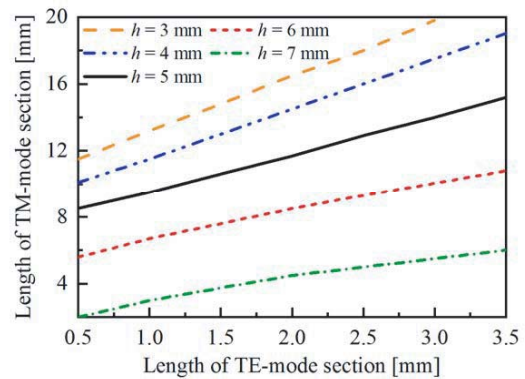


**Figure 8.** Relation between the lengths of the TE and the TM sections for various ridge heights  $h$  under the balanced condition.

depending on the ridge height  $h$  beyond the cutoff frequency of the  $TM_{01}$  mode insensitive to  $h$ . Fig. 7 shows the transmission characteristic for 12 unit cells of the structure fulfilling the balanced condition. The passband starts from around 8.7 GHz in the left-handed region and smoothly continues to the right-handed region, keeping low insertion loss.

We next investigate effect of the length of TE-mode and TM-mode sections under the balanced condition for various heights of the ridge  $h$ . Fig. 8 shows the relation between the lengths  $l_1$  and  $l_2$  for the fixed value  $h$  that fulfills the balanced condition. Using this figure, we can see at a glance that the band gap exists between the two passband regions in the guide structures not lying on the given curves.

#### 4. EXPERIMENTAL RESULTS

We have fabricated the proposed waveguide with ridge height  $h = 4.5$  [mm] for 12 and 30 unit cells and measured their transmission characteristics by the vector network analyzer (Agilent Technologies Inc. E8361C). The photographs shown in Figs. 9(a) and (b) are the whole structure of the fabricated CRLH cylindrical waveguide and its cross section of the TE-waveguide part ( $w = 3$  [mm] and  $d = 2$  [mm]). Fig. 10 shows the inside structure of the coaxial exciter. The length of the TE waveguide is  $l_1 = 1.0$  [mm], and the length of the TM waveguide is  $l_2 = 10.0$  [mm] (It should be noted that the length of the

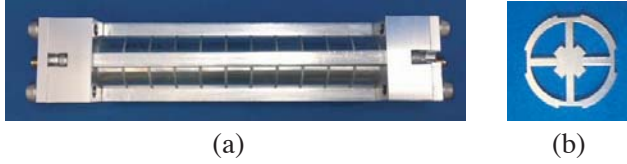


**Figure 9.** Photographs of (a) the whole structure of the fabricated CRLH cylindrical waveguide and (b) its cross section of the TE-waveguide part.

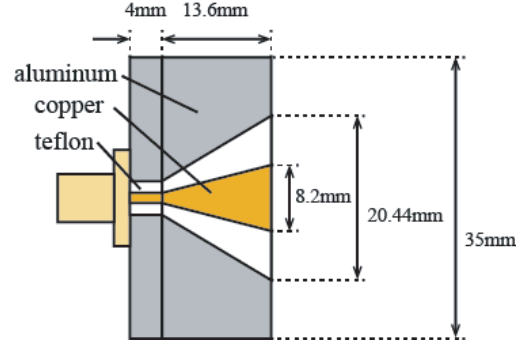


**Figure 10.** Inside structure of the coaxial exciter.

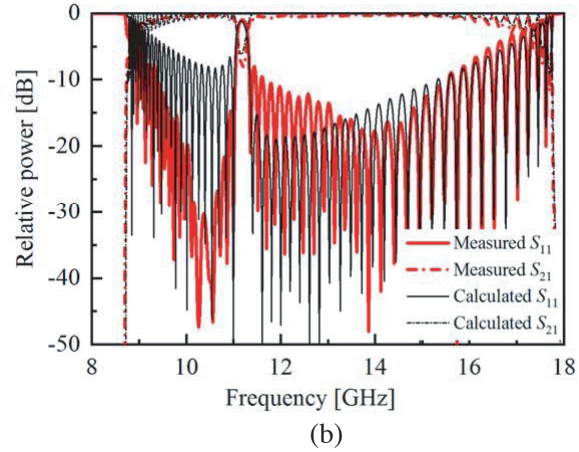
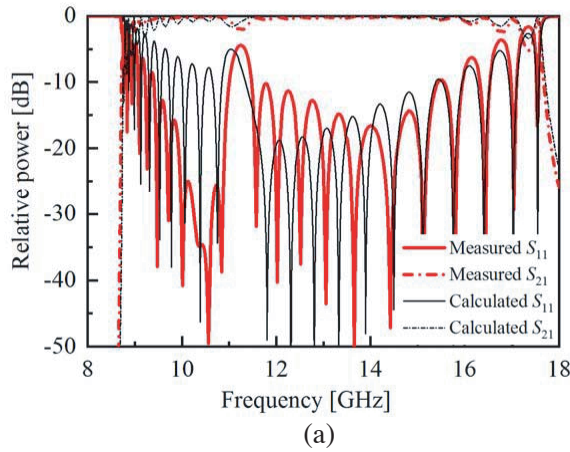


**Figure 11.** Comparison of the measured transmission characteristics for (a) 12 and (b) 30 cells with the calculated ones.

TM waveguide of input/output ports is  $l_2/2 = 5$  [mm].) Figs. 11(a) and (b) compare the transmission characteristics for 12 and 30 cells between the calculated and measured results. In the calculated results, the uniform coaxial line (the outer radius is the same as that of the fabricated CRLH-TL) is considered as the coaxial exciter, while the measured results are obtained by using the taper coaxial exciter shown in Fig. 10. Furthermore, the fabricated CRLH-TL is made up by stacking pieces of the TM-mode and TE-mode sections one by one along four guides cut along an outer wall of the circumference (see Fig. 9), so that the precision of the guide dimension is not so high. You can see a slight difference between the reflected characteristics in the frequency near the gap band for these reasons, but the overall filter characteristics fairly agree with each other, and also the passbands obtained by both results are located in almost the same frequency range. Therefore, it has been verified experimentally that the proposed structure works well as a CRLH waveguide.

## 5. CONCLUSION

We have proposed the right/left-handed composite cylindrical waveguide which is constructed by the cutoff TM-mode section and cutoff TE-mode section. In the latter section, the 4-divided ridge-loaded sector waveguide is successfully introduced to match the field distributions between the two modes and to adjust the cutoff frequency of the TE-mode. Usefulness of the proposed composite waveguide has been verified from dispersion diagrams and transmission characteristic for the finite-number of the unit cells.

## ACKNOWLEDGMENT

This work was supported in part by a Grant-in-Aid for Scientific Research (C) (16K06372) from Japan Society for the Promotion of Science.

## REFERENCES

1. Veselago, V., "The electrodynamics of substrates with simultaneously negative values of  $\epsilon$  and  $\mu$ ," *Soviet Physics Uspekhi*, Vol. 10, No. 4, 509–514, 1968.
2. Smith, D. R., W. J. Padilla, D. C. Vier, S. C. Nemat-Nasser, and S. Schultz, "Composite medium with simultaneously negative permeability and permittivity," *Phys. Rev. Lett.*, Vol. 84, 4184–4187, May 2000.
3. Alzan, V., et al., "Tailoring the physical properties of nanocomposite films by the insertion of graphene and other nanoparticles," *Compos. Part B: Eng.*, Vol. 60, 29–35, Apr. 2014.
4. Gugliuzza, A., A. Politano, and E. Drioli, "The advent of graphene and other two-dimensional materials in membrane science and technology," *Curr. Opin. Chem. Eng.*, Vol. 16, 78–85, May 2017.
5. Caloz, C. and T. Itoh, "Transmission line approach of left-handed (LH) materials and microstrip implementation of an artificial LH transmission line," *IEEE Trans. Antennas Propagat.*, Vol. 52, No. 5, 1159–1166, May 2004.
6. Ikeda, T., K. Sakakibara, T. Matsui, N. Kikuma, and H. Hirayama, "Beam-scanning performance of leaky-wave slot-array antenna on variable stub-loaded left-handed waveguide," *IEEE Trans. Antennas Propagat.*, Vol. 56, No. 12, 3611–3618, Dec. 2008.
7. Kim, D. J. and J. H. Lee, "Beam scanning leaky-wave slot Antenna using balanced CRLH waveguide operating above the cutoff frequency," *IEEE Trans. Antennas Propagat.*, Vol. 61, No. 5, 2432–2440, May 2013.
8. Eshrah, I. A., A. A. Kishk, A. B. Yakovlev, and A. W. Glisson, "Rectangular waveguide with dielectric-filled corrugations supporting backward waves," *IEEE Trans. Microwave Theory Tech.*, Vol. 53, No. 11, 3298–3304, Nov. 2005.
9. Iwasaki, T., H. Kamoda, T. Derham, and T. Kuki, "A composite right/left-handed rectangular waveguide with tilted corrugations for millimeter-wave frequency scanning antenna," *2008 European Microwave Conf.*, 563–566, Amsterdam, Oct. 2008.
10. Kord, A. M. and I. A. Eshrah, "Generalised asymptotic boundary conditions and their application to composite right/left-handed rectangular waveguide with double-ridge corrugations," *IET Microwaves, Antennas Propagat.*, Vol. 8, No. 13, 1014–1020, Oct. 2014.
11. Semouchkina, E., S. Muduruni, G. Semouchkin, and R. Mittra, "Band-pass filtering by below-cutoff waveguides loaded with split-ring resonators: Relevance to lefthandedness," *2007 IEEE MTT-S Intern'l Symp.*, 1839–1842, Honolulu, HI, Jun. 2007.
12. Eldeen, A. M. N. and I. A. Eshrah, "CRLH waveguide with air-filled double-ridge corrugations," *2011 IEEE AP-S Intern'l Symp.*, 2965–2968, Spokane, WA, Jul. 2011.
13. Mizutani, Y., M. Kishihara, I. Ohta, K. Okubo, and H. Takimoto, "Constitution of left-handed waveguide using cutoff TM mode," *2014 APMC*, 208–210, Sendai, Japan, Nov. 2014.
14. Oshima, I., T. Seki, N. Michishita, and K. Cho, "Omnidirectional composite right/left-handed leaky-wave antenna with downtilted beam," *2015 IEEE AP-S Intern'l Symp.*, 2439–2440, Vancouver, BC, Jul. 2015.
15. Sakamoto, A., K. Cho, N. Michishita, T. Seki, and I. Oshima, "Transmission characteristic comparison between right and left handed leaky wave antennas composed of CRLH coplanar strip line," *2016 ISAP*, 828–829, Okinawa, Oct. 2016.
16. Mohan, M. P. and A. Alphones, "Double periodic CRLH transmission line for wideband performance," *2016 APMC*, 1–4, New Delhi, Dec. 2016.
17. Yang, Q., X. Zhao, and Y. Zhang, "Leaky-wave radiation analysis for CRLH waveguide with long slot on its broadwall," *EuCAP 2016*, 1–5, Davos, Apr. 2016.

18. Siaka, F., J. J. Laurin, and R. Deban, "New broad angle frequency scanning antenna with narrow bandwidth based on a CRLH structure," *IET Microwaves, Antennas Propaga.*, Vol. 11, No. 11, 1644–1650, Sep. 2017.
19. Siddiqui, Z., A. Radwan, M. Sonkki, M. Tuhkala, and S. Myllymäki, "Leaky coaxial cable antenna based on sinusoidally-modulated reactance surface," *2017 Progress In Electromagnetics Research Symposium — Spring (PIERS)*, 3887–3890, St Petersburg, Russia, May 22–25, 2017..
20. Yuki, M., M. Kishihara, and I. Ohta, "Constitution of left-handed waveguide based on cutoff TE- and TM-mode," *IEICE Transactions on Electronics (Japanese Edition)*, C-2-67, May 2014.
21. Nishimura, S., H. Deguchi, and M. Tsuji, "Radiation characteristics in new CRLH cylindrical waveguides," *2015 APCAP*, 350–352, Bali Island, Indonesia, Jul. 2015.
22. Nishimura, S., H. Deguchi, and M. Tsuji, "Transmission characteristic on a partially ridge-loaded composite right/left-handed cylindrical waveguide," *2015 ICEAA Intern'l Conf.*, 844–846, Torino, Italy, Sep. 2016.
23. Nishimura, S., H. Deguchi, and M. Tsuji, "Radiation characteristics of leaky-wave antenna using ridge-loaded composite right/left-handed cylindrical waveguides," *2016 IEEE AP-S Intern'l Symp.*, 85–86, Fajardo, Oct. 2016.
24. Uyama, K., S. Nishimura, H. Deguchi, and M. Tsuji, "Transmission characteristics of CRLH rectangular waveguides constructed by the cutoff modes of TM and TE waves," *2016 ICEAA Intern'l Conf.*, 728–731, Cairns, Australia, Sep. 2016.
25. Mukainoge, Y., H. Deguchi, and M. Tsuji, "An optimized design method of composite right/left handed transmission lines considering higher-order mode interaction by genetic algorithm," *2014 IEEE Intern. Workshop on Electromagnetics*, 78–79, Aug. 2014.